

# Unveiling the sea: universality of the transverse momentum dependent quark distributions at small $x$

Paul Caucal,<sup>1,\*</sup> Marcos Guerrero Morales,<sup>2,†</sup> Edmond Iancu,<sup>3,‡</sup> Farid Salazar,<sup>2,4,5,6,§</sup> and Feng Yuan<sup>7,3,¶</sup>

<sup>1</sup>*SUBATECH UMR 6457 (IMT Atlantique, Université de Nantes, IN2P3/CNRS), 4 rue Alfred Kastler, 44307 Nantes, France*

<sup>2</sup>*Department of Physics, Temple University, Philadelphia, PA 19122 - 1801, USA*

<sup>3</sup>*Université Paris-Saclay, CNRS, CEA, Institut de physique théorique, F-91191, Gif-sur-Yvette, France*

<sup>4</sup>*RIKEN-BNL Research Center, Brookhaven National Laboratory, Upton, New York 11973, USA*

<sup>5</sup>*Physics Department, Brookhaven National Laboratory, Upton, New York 11973, USA*

<sup>6</sup>*Institute for Nuclear Theory, University of Washington, Seattle WA 98195-1550, USA*

<sup>7</sup>*Nuclear Science Division, Lawrence Berkeley National Laboratory, Berkeley, CA 94720, USA*

Within the Colour Glass Condensate effective theory, we demonstrate that back-to-back dijet correlations in dilute-dense collisions involving a small- $x$  quark from the nuclear target can be factorised in terms of universal transverse momentum dependent distributions (TMDs) for the sea quarks. Two building blocks are needed to construct all these TMDs at the operator level: the sea quark TMD operator which appears in semi-inclusive Deep-Inelastic Scattering (SIDIS) or in the Drell-Yan process and the elastic  $S$ -matrix for a quark-antiquark dipole. Compared to SIDIS, the saturation effects are stronger for dijet production in forward proton-nucleus collisions, due to additional scattering in the initial and final state, effectively resulting in a larger value for the nuclear saturation momentum.

*Introduction.* One of the key insights from the high-energy electron-proton collisions at HERA is the rapid rise of the gluon distribution in protons as the longitudinal momentum fraction  $x$  of the gluon with respect to the proton decreases [1]. This steep growth is moderated by non-linear gluon saturation, an emergent phenomenon described by the Colour Glass Condensate (CGC) effective theory [2–6]. The experimental characterisation of gluon saturation is a central objective of the future Electron-Ion Collider (EIC) [7–9], which will extend the groundbreaking work of HERA [10, 11]. On the other hand, HERA also showed [12, 13] that the proton wave-function at small  $x$  contains a substantial component of “sea” quarks, which arise primarily from quark-antiquark pair production from small- $x$  gluons. In this Letter, we demonstrate that the CGC consistently accounts for the sea quark contribution [14–16] inside nuclei and predicts the shape of the quark transverse momentum dependent (TMD) distributions [17, 18] in the saturation regime.

Our analysis builds upon pioneering work which unveiled sea quark TMD factorisation for selected processes in electron-nucleus ( $eA$ ) deep inelastic scattering (DIS) at small  $x$ : the semi-inclusive production (SIDIS) of quark jets (or hadrons) [19–21], lepton-jet correlations [22], and the diffractive production of quark jets [23] and of quark-gluon dijets [24]. Despite such interesting, but rare, examples, a systematic understanding of the emergence of quark TMD factorisation at small  $x$  — similar to that for the case of gluons [25–50] — was still missing. It is our purpose in this Letter to fill this gap. Via the study of representative processes describing inclusive two-particle production (dijets, dihadrons, or photon-jets, to be collectively referred to as “dijets” in what follows) in  $eA$  DIS and proton-nucleus ( $pA$ ) collisions,

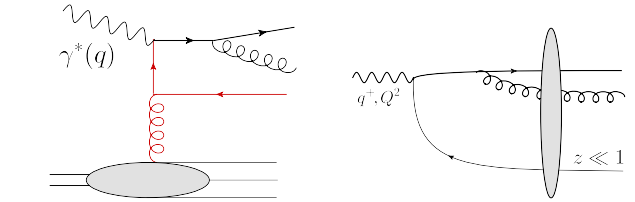


Figure 1. Graphs contributing to quark-gluon production in DIS at small  $x$  and to leading order. Right: target picture (photon absorbed by a sea quark). Left: CGC picture (a  $q\bar{q}g$  fluctuation of the photon scatters off the shockwave target field).

we will demonstrate the ubiquitousness and the universality of the sea quark TMDs, as computed from the CGC.

The dijet processes of interest for us here involve a hard scattering between a parton from the dilute projectile and a sea quark with  $x \ll 1$  from the nuclear target, hence they are suppressed by a power of the QCD coupling  $\alpha_s$  compared to gluon-mediated processes leading to similar final states. Yet, since the sea quark distribution is driven by that of the small- $x$  gluons, these processes show exactly the same behaviour at high energy as their gluonic counterparts. So, their contributions must be taken into account for the phenomenology of back-to-back two-particle correlations at high energies, as probed via forward particle production in  $pA$  collisions at the Large Hadron Collider, or in  $eA$  collisions at the EIC. Since the sea quark TMD is sensitive to gluon saturation [14–16] (see also below), our results open a new window for saturation studies at colliders through the quark channel.

To be more specific, consider quark-gluon dijet production in DIS, as illustrated (within the standard par-

ton picture for the target) by the left Feynman graph in Fig. 1. The dijets are assumed to be hard and nearly back-to-back in the transverse plane: their relative transverse momentum  $P_\perp$  is much larger than both their momentum imbalance  $K_\perp$  and the target saturation momentum  $Q_s(x)$ . Despite being hard, the dijets can probe low- $x$  partons in the target wavefunction provided the center-of-mass (COM) energy is sufficiently high and that, in the COM frame, the jets are produced at forward rapidities, in the fragmentation region of the dilute projectile.

Below, we shall compute the dijet cross-section in the CGC effective theory, to leading order (LO) in  $\alpha_s$  and to leading powers (LP) in the small ratios  $K_\perp/P_\perp$  and  $Q_s/P_\perp$ . We shall thus find *TMD factorisation*: to the accuracy of interest, the cross-section is the product between a *hard factor* (the same as for the corresponding processes at moderate  $x$ , see e.g. [51]) and a *sea quark TMD*, for which the CGC approach offers explicit results from first principles.

As we shall see, there are multiple such sea quark TMDs, depending upon the process. Yet, they share a universal structure determined by the colour flow of the hard partonic process. At the operator level, this universal structure reflects the various possible gauge links connecting bilocal quark field operators [52]. In the multicolour limit  $N_c \rightarrow \infty$ , all the emerging TMDs are built with only two ingredients: the sea quark TMD from the CGC calculation of SIDIS [19] and a colour dipole operator describing initial-state and final-state interactions in the eikonal approximation.

*Target vs. projectile picture.* TMD (or collinear) factorisation is traditionally formulated in the target parton picture, where the small- $x$  quark that is knocked out by the collision is a constituent of the target — the quark component of a sea quark-antiquark ( $q\bar{q}$ ) pair. The CGC picture is however different. The target is described as a classical colour field (a “shockwave”) representing the small- $x$  gluons, but there are no explicit quark degrees of freedom: valence quarks are implicitly included as sources for the colour fields, but the sea quarks are absent<sup>1</sup>. In the CGC picture, the would-be *scattering* between a parton from the projectile and a sea quark from the target is instead described as the *emission* of a soft *antiquark* by the projectile parton. This antiquark participates in the scattering with the target colour field, but it is not measured in the final state. Thus, the CGC calculation of dijet production requires the study of a three-parton Fock component of the light-cone (LC) wavefunction (WF) of the projectile (see the right graph

in Fig. 1 for an example). To that aim, the calculation should be performed in a Lorentz frame where the projectile is ultrarelativistic and in the projectile LC gauge.

Let us consider the DIS process in Fig. 1 for definiteness. The CGC factorisation for this process, a.k.a. the colour dipole picture (CDP) [56–59], is formulated in a frame where the virtual photon is a right-mover with 4-momentum  $q^\mu = (q^+, q^- = -Q^2/2q^+, \mathbf{0}_\perp)$  with  $q^+ \gg Q$ , while the nuclear target is a left mover with  $P_N^\mu \simeq \delta^{\mu-} P_N^-$  per nucleon. The photon LCWF is constructed in perturbation theory, in the LC gauge  $A_a^+ = 0$ . To compute quark-gluon ( $qg$ ) dijet production to LO, one needs the 3-parton Fock state  $q\bar{q}g$ . Introducing LC longitudinal momenta  $k_i^+ \equiv z_i q^+$  and transverse momenta  $\mathbf{k}_i$  for the three partons ( $i = q, \bar{q}, g$ ), the dijet transverse relative momentum and imbalance are defined as  $\mathbf{P} = z_g \mathbf{k}_q - z_q \mathbf{k}_g$  and  $\mathbf{K} = \mathbf{k}_q + \mathbf{k}_g$ , respectively, with  $K_\perp \ll P_\perp$  in the back-to-back limit. To simplify notations, we shall use  $z$  and  $\mathbf{k}$  (instead of  $z_{\bar{q}}, \mathbf{k}_{\bar{q}}$ ) for the unmeasured antiquark.

To uncover TMD factorisation for  $qg$  dijets, we isolate the LP in the ratio  $K_\perp/P_\perp$  and integrate out the kinematics ( $z, \mathbf{k}$ ) of the unmeasured antiquark. This integration is controlled by transverse momenta  $k_\perp \sim K_\perp$  and small values  $z \sim K_\perp^2/P_\perp^2 \ll 1$  for the longitudinal momentum fraction. This can be understood from a formation time argument: in a hard process, the antiquark formation time  $\Delta x^+ \sim zq^+/k_\perp^2$  is comparable to that of the hard  $qg$  pair:

$$\frac{zq^+}{K_\perp^2} \sim \frac{z_q z_g q^+}{P_\perp^2} \Rightarrow z \sim \frac{K_\perp^2}{P_\perp^2}. \quad (1)$$

Thus, importantly, the unmeasured antiquark in the CGC picture (the same as the struck sea quark in the target picture) is *soft* both w.r.t. to the projectile,  $z \ll 1$ , and w.r.t. the target,  $x \ll 1$ . Being soft, it can indeed be “transferred” between the projectile and the target, as explained in [21, 24, 42, 49, 50, 60].

This special kinematics for the three parton system also implies a special geometry for the collision in the transverse plane, as suggested by our drawing of the CGC graph in Fig. 1: the hard  $qg$  pair has a small size  $r \sim 1/P_\perp \ll 1/Q_s$  and is separated from the soft antiquark by a large distance  $R \sim 1/K_\perp \gg r$ . Accordingly, the incoming photon, the intermediate quark, and the hard  $qg$  dijet are all aligned with each other: the respective transverse coordinates are roughly the same.

*Quark-gluon dijet production in  $eA$  DIS.* Let us now compute the cross-section for the CGC process  $\gamma^* + A \rightarrow qg(\bar{q}) + X$ . In general, there are two possible topologies: gluon emission by the quark (cf. Fig. 1), or by the antiquark (see Fig. 2). For a photon with transverse polarisation ( $\gamma_T^*$ ), both topologies contribute on the same footing, but for a longitudinal one ( $\gamma_L^*$ ), the first possibility is suppressed. (Indeed, in that case, the photon splitting

<sup>1</sup> Fermionic background fields can be introduced via sub-eikonal corrections to the scattering. This has been used to study quark TMD factorisation in dilute-dense collisions [53–55]. In this approach, the quark TMDs are not explicitly computed, but merely related to formal correlation functions of the fermionic background field.

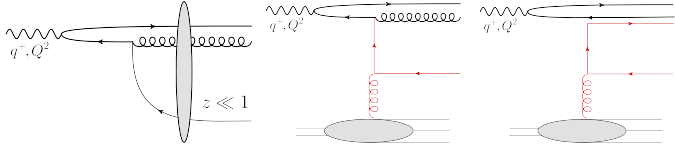


Figure 2. Left: CGC picture for back-to-back quark-gluon dijets in  $\gamma_L^* A$  collisions. Middle: The corresponding target picture. Right: The associated colour flow at large  $N_c$ .

function  $\gamma_L^* \rightarrow q\bar{q}$  is proportional to  $z(1-z) \ll 1$ .) For simplicity, we present details only for  $\gamma_L^*$  and defer the discussion of  $\gamma_T^*$  to a forthcoming publication.

To LP in  $K_\perp/P_\perp$ , the amplitude for gluon emission by the antiquark is obtained as

$$\mathcal{M}_{q\bar{q}(g)}^{\lambda\sigma\bar{\sigma}} = 8ee_f g \sqrt{z_q z_g} \delta^{\sigma, -\bar{\sigma}} \delta^{\lambda\sigma} \frac{Q}{M_{qg}^2 + Q^2} \quad (2)$$

$$\times \int \frac{d^2\ell}{(2\pi)^2} \frac{\ell \cdot \epsilon^{\lambda*}}{\ell^2 + z(Q^2 + M_{qg}^2)} C_1^a(\mathbf{K} - \ell, \ell + \mathbf{k}),$$

where  $M_{qg}^2 \equiv (k_q + k_g)^2 \simeq P_\perp^2/(z_q z_g)$ ,  $\lambda$  and  $a$  refer to the transverse polarisation and the colour of the produced gluon,  $\sigma$  and  $\bar{\sigma}$  are helicity indices for the quark and antiquark,  $g$  and  $e$  denote the strong and electromagnetic charges, and  $e_f$  is the fractional electric charge of a quark with flavour  $f$ . Eq. (2) involves the colour operator

$$C_1^a(\mathbf{q}_1, \mathbf{q}_2) = \int_{\mathbf{x}, \mathbf{y}} e^{-i\mathbf{q}_1 \cdot \mathbf{x} - i\mathbf{q}_2 \cdot \mathbf{y}} t^a [V_{\mathbf{x}} V_{\mathbf{y}}^\dagger - 1], \quad (3)$$

with  $V_{\mathbf{x}}$  a light-like Wilson line in the fundamental representation of  $SU(N_c)$  with fixed transverse coordinate  $\mathbf{x}$ . The Wilson lines in Eq. (3) describe the scattering of the effective  $q\bar{q}$  dipole, where the ‘‘quark’’ truly is the small  $qg$  pair. The colour matrix  $t^a$  refers to the gluon emission. By removing this matrix and replacing  $g \rightarrow -ee_f$  in Eq. (2), one gets the amplitude for  $\gamma q\bar{q}$  production in DIS; hence this paragraph also encompasses  $\gamma$ -jet correlations in DIS [61].

To get the quark-gluon dijet cross-section, one must square this amplitude and integrate over the soft antiquark phase space, i.e. over  $\mathbf{k}$  and  $z$ . After also extracting the LP in  $K_\perp/P_\perp$ , one finds

$$\frac{d\sigma^{\gamma_L^* A \rightarrow qg+X}}{d^2\mathbf{P} d^2\mathbf{K} dz_q dz_g} = \delta(1 - z_q - z_g) \frac{8\alpha_{\text{em}} e_f^2 \alpha_s Q^2}{z_g (Q^2 + M_{qg}^2)^3} \quad (4)$$

$$\times C_F xq^{(1)}(x, \mathbf{K}).$$

This result is leading twist since the hard factor in the first line behaves like  $1/P_\perp^4$  when  $P_\perp^2 \sim Q^2$ . As expected, this is the same as the hard factor in the collinear factorisation result for the partonic process  $\gamma_L^* q \rightarrow qg$ .

Eq. (4) demonstrates TMD factorisation with an explicit result for the sea quark TMD, conveniently written

as  $xq^{(1)}(x, \mathbf{K}) \equiv \langle \mathcal{Q}(\mathbf{K}) \rangle_x$ , where the brackets  $\langle \dots \rangle_x$  refer to the CGC average over the target colour fields and the sea quark operator  $\mathcal{Q}$

$$\mathcal{Q}(\mathbf{K}) \equiv \frac{N_c}{4\pi^4} \int_{\mathbf{b}, \mathbf{q}} \mathcal{D}_F^{(1)}(\mathbf{b}, \mathbf{q}) \quad (5)$$

$$\times \left[ 1 - \frac{\mathbf{K} \cdot (\mathbf{K} - \mathbf{q})}{K_\perp^2 - (\mathbf{K} - \mathbf{q})^2} \ln \left( \frac{K_\perp^2}{(\mathbf{K} - \mathbf{q})^2} \right) \right],$$

involves the dipole operator  $\mathcal{D}_F^{(n=1)}(\mathbf{b}, \mathbf{q})$ , defined as (for arbitrary integer  $n$ , for later convenience)

$$\mathcal{D}_F^{(n)}(\mathbf{b}, \mathbf{q}) \equiv \int_{\mathbf{r}} \frac{e^{-i\mathbf{q} \cdot \mathbf{r}}}{(2\pi)^2} \left( \frac{1}{N_c} \text{Tr} [V_{\mathbf{b}+\mathbf{r}/2} V_{\mathbf{b}-\mathbf{r}/2}^\dagger] \right)^n. \quad (6)$$

This operator depends upon the impact parameter  $\mathbf{b}$  of the  $q\bar{q}$  dipole and the transverse momentum  $\mathbf{q}$  transferred by the target via the collision. Transverse momentum conservation shows that the difference  $\mathbf{q} - \mathbf{K}$  is the momentum of the unmeasured antiquark.

The  $x$  dependence of the quark TMD  $xq^{(1)}(x, \mathbf{K})$  is controlled by the BK/JIMWLK [62–70] evolution of  $\mathcal{D}_F^{(1)}$  down to  $x = x_{qg}$ , with  $x_{qg}$  the target longitudinal fraction taken by the measured dijet. This is obtained from the condition of LC energy ( $k^-$ ) conservation as  $x_{qg} = (M_{qg}^2 + Q^2)/\hat{s}$  with  $\hat{s} = (P + q)^2$ .

The quark TMD  $xq^{(1)}(x, \mathbf{K})$  is identical to that obtained in the CGC calculation of SIDIS at small  $x$  [19, 20]. This is consistent with the fact that the colour flow is identical for both processes, due to the small transverse size of the hard dijet. This flow is illustrated in Fig. 2 in the large  $N_c$  limit. (The  $q\bar{q}$  dipole which is disconnected from the quark TMD has a negligible transverse size  $r \sim 1/P_\perp$ , so it does not contribute to the colour flow.) Eq. (5) has a natural interpretation in the target picture [71]:  $\mathbf{q}$  is the transverse momentum of the parent gluon which generates the  $q\bar{q}$  sea pair, while

$$xG^{(2)}(x, \mathbf{q}) \equiv \frac{q_\perp^2 N_c}{2\pi^2 \alpha_s} \int_{\mathbf{b}} \langle \mathcal{D}_F^{(1)}(\mathbf{b}, \mathbf{q}) \rangle_x, \quad (7)$$

represents the dipole unintegrated gluon distribution (UGD). As discussed in [25, 26], this distribution plays the role of a TMD for small- $x$  processes which involve both initial-state and final-state interactions, i.e. which feature coloured partons on both the incoming and the outgoing legs. Of course, this is not the case in DIS, where all the coloured partons are outgoing. Yet, the dipole UGD is relevant in this context since the gluon distribution of the target is ‘‘probed’’ by a  $q\bar{q}$  sea pair and the antiquark in this pair mimics an incoming quark in the initial state. This suggests that the second line of Eq. (5) times  $\alpha_s/q_\perp^2$  can be interpreted as a *transverse momentum dependent gluon-to-quark splitting function* (integrated over the splitting fraction  $\xi$ ). It indeed coincides with the off-shell splitting function employed in  $k_T$ -factorisation [72–75]. A more complete result, where the  $\xi$ -dependence is visible, can be found in [20, 71].

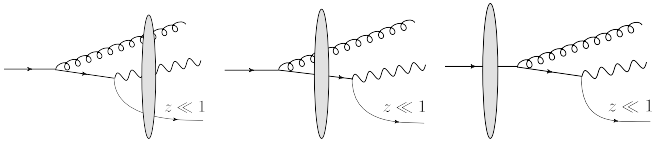


Figure 3. Feynman graphs for  $qA \rightarrow \gamma g(q) + X$  amplitudes at small  $x$  in the CGC ( $\gamma \leftrightarrow g$  exchanged diagrams not shown).

*Photon-quark dijets in quark-initiated  $pA$  collisions.* We now consider inclusive back-to-back photon-jet production in forward  $pA$  collisions in the channel  $qA \rightarrow \gamma g(q) + X$ . That is, the scattering is initiated by a quark from the proton (assumed to be on-shell prior to the collision) and the hadronic “jet” in the final state corresponds to a gluon — so the final quark (with kinematical variables  $z$  and  $\mathbf{k}$ ) is soft and unmeasured:  $k_\perp \sim K_\perp$  and  $z \sim K_\perp^2/P_\perp^2 \ll 1$ . The relevant CGC amplitudes are shown in Fig. 3. As before, the total amplitude drastically simplifies after keeping only the LP in  $K_\perp/P_\perp$ , and reads

$$\begin{aligned} \mathcal{M}_{\gamma g(q)}^{\bar{\lambda}\lambda\sigma\sigma'} &= 8e e_f g \sqrt{z} q^+ \delta^{\sigma\sigma'} \delta^{\sigma, -\lambda} \left[ \delta^{\lambda\bar{\lambda}} + z_\gamma \delta^{\lambda, -\bar{\lambda}} \right] \\ &\times \frac{\mathbf{P} \cdot \boldsymbol{\epsilon}^{\bar{\lambda}*}}{\mathbf{P}^2} \int \frac{d^2\ell}{(2\pi)^2} \left[ \frac{\boldsymbol{\ell} \cdot \boldsymbol{\epsilon}^{\lambda*}}{\ell^2 + z M_{\gamma g}^2} + \frac{\mathbf{k} \cdot \boldsymbol{\epsilon}^{\lambda*}}{\mathbf{k}^2 + z M_{\gamma g}^2} \right] \\ &\times \mathcal{C}_2^a(\boldsymbol{\ell} + \mathbf{k}, \mathbf{K} - \boldsymbol{\ell}) + (\gamma \leftrightarrow g), \end{aligned} \quad (8)$$

where  $\sigma, \sigma', \lambda, \bar{\lambda}$  respectively refer to the incoming and outgoing quark helicities and to the photon and gluon polarisation,  $a$  to the colour of the gluon, and  $M_{\gamma g}$  is the  $\gamma$ -jet invariant mass. The first (second) term inside the square brackets corresponds to gluon emission before (after) the shockwave. In the first case, the gluon participates in the scattering as well, so the respective amplitude involves the colour operator

$$\mathcal{C}_2^a(\mathbf{q}_1, \mathbf{q}_2) = \int_{\mathbf{x}, \mathbf{z}} e^{-i\mathbf{q}_1 \cdot \mathbf{x} - i\mathbf{q}_2 \cdot \mathbf{z}} V_{\mathbf{x}} t^b U_{\mathbf{z}}^{ab}, \quad (9)$$

(with  $U_{\mathbf{z}}^{ab}$  an adjoint Wilson line) describing the scattering of quark-gluon system off the strong gluon field of the target. For the second term, the integral over  $\ell$  yields a  $\delta$ -function enforcing  $\mathbf{x} = \mathbf{z}$  which simplifies the colour operator as follows  $V_{\mathbf{x}} t^b U_{\mathbf{z}}^{ab} \rightarrow t^a V_{\mathbf{x}}$ ; as expected, this describes the scattering of the quark probe alone.

Squaring this amplitude and integrating over the kinematic  $(z, \mathbf{k})$  of the unmeasured quark gives the inclusive  $\gamma$ +gluon-jet cross-section in the leading-twist approximation of interest

$$\begin{aligned} \frac{d\sigma^{qA \rightarrow \gamma g + X}}{d^2\mathbf{P} d^2\mathbf{K} dz_\gamma dz_g} &= \delta(1 - z_\gamma - z_g) \frac{\alpha_{\text{em}} e_f^2 \alpha_s (z_\gamma^2 + z_g^2)}{N_c \mathbf{P}^4} \\ &\times \left[ \frac{N_c}{2} xq^{(2)}(x, \mathbf{K}) - \frac{1}{2N_c} xq^{(1)}(x, \mathbf{K}) \right], \end{aligned} \quad (10)$$

where  $x = x_{\gamma g}$ . The first term, which is the only one to survive at large  $N_c$ , features a new quark TMD operator

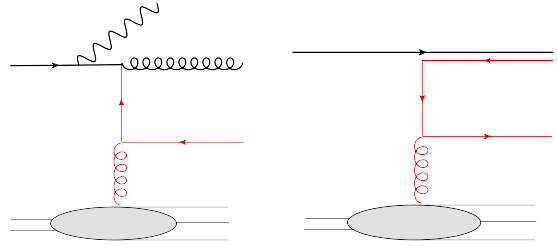


Figure 4. Left: Target picture for  $\gamma g$  jets in  $pA$  collisions. Right: The associated colour flow at large  $N_c$ .

at small  $x$ , defined as a convolution between our previous sea quark TMD operator  $\mathcal{Q}(\mathbf{b}, \mathbf{K})$  (the version of the operator in Eq. (5) at a fixed value of the impact parameter  $\mathbf{b}$ ) and the dipole operator  $\mathcal{D}_F^{(1)}(\mathbf{b}, \mathbf{q})$  (cf. Eq. (6)):

$$xq^{(2)}(x, \mathbf{K}) = \int_{\mathbf{b}, \mathbf{q}} \left\langle \mathcal{D}_F^{(1)}(\mathbf{b}, \mathbf{q}) \mathcal{Q}(\mathbf{b}, \mathbf{K} - \mathbf{q}) \right\rangle_x. \quad (11)$$

The target picture for this process and the associated colour flow at large  $N_c$  are illustrated in Fig. 4. These figures make clear that the overall process involves both initial and final state interactions. After replacing the gluon by a point-like  $q\bar{q}$  pair (as appropriate at large  $N_c$ ), the ensemble of these interactions can be resummed into a fundamental Wilson line extending from  $x^+ \rightarrow -\infty$  to  $x^+ \rightarrow \infty$ , which factorises from the rest of the amplitude. This infinite Wilson line has a fixed transverse coordinate since the incoming quark and the outgoing gluon have roughly the same transverse positions. Its product with the hermitian conjugate Wilson line from the complex conjugate amplitude yields the dipole operator visible in Eq. (11). This can be recognised as a *Wilson loops* (since the transverse fields vanish at  $x^+ \rightarrow \pm\infty$ ), whose appearance was to be expected: such Wilson loop are well known to enter the gauge link structure of the operators defining quark TMDs in processes with both initial and final state interactions [52].

*Gluon-quark dijets in gluon-initiated  $pA$  collisions.* Our last example refers to gluon-quark dijets in  $pA$  collisions via the  $gq \rightarrow gq$  hard process, which in the CGC calculation looks like  $g + A \rightarrow qg(\bar{q}) + X$ .

Besides the DIS-like diagrams where the gluon is emitted by the quark or the antiquark, cf. Figs. 1 and 2, there is an additional topology which involves the triple gluon vertex, see Fig. 5. At large  $N_c$ , there are two patterns for the colour flow associated with this topology: one where the quark component of the incoming gluon is transmitted to the outgoing gluon, and one where this component becomes the produced quark. In both cases, this quark component gives rise to an infinite Wilson line which generates a Wilson loop (or dipole correlator) in the cross-section. In the second pattern though, there is another such a Wilson line, associated with the antiquark component of the original gluon. Hence, the

cross-section generated by this topology will feature two types of sea quark TMDs: one with a single Wilson loop, as shown in Eq. (11), and another one involving two Wilson loops which in the transverse plane lie on top of each other. (Indeed, in the approximations of interest, the incoming gluon and the two produced jets roughly have the same transverse coordinate.)

The colour flows depicted in Fig. 5 also reveals an interesting structure for the sea quark operator. In the first pattern, the (effective) colour flow corresponds to *initial-state interactions*; hence, the corresponding version of the operator  $\mathcal{Q}(\mathbf{b}, \mathbf{K})$  is the one that would naturally enter the Drell-Yan process ( $q\bar{q} \rightarrow \gamma^* \rightarrow \ell^+\ell^- + X$ ) in  $pA$  collisions [20]. For an unpolarised target, this coincides with the respective SIDIS operator in Eq. (5). In the second pattern, we recover the original SIDIS operator  $\mathcal{Q}(\mathbf{b}, \mathbf{K})$ , with a colour flow encoding final-state interactions.

The total amplitude at LP in  $K_\perp/P_\perp$  taking into account all possible topologies can be found in the Appendix. The final CGC result for the back-to-back  $qg$  dijet cross-section is found as (in the large  $N_c$  limit)

$$\frac{d\sigma^{gA \rightarrow gq+X}}{d^2\mathbf{P}d^2\mathbf{K}dz_qdz_g} = \delta(1-z_q-z_g) \frac{\alpha_s^2(1+z_g^2)}{2z_q\mathbf{P}^4} \times \left[ xq^{(3)}(x, \mathbf{K}) + z_g^2 xq^{(2)}(x, \mathbf{K}) \right], \quad (12)$$

where the quark TMDs are defined for generic integer  $n \geq 1$  by the following generalisation of Eq. (11):

$$xq^{(n)}(x, \mathbf{K}) = \int_{\mathbf{b}, \mathbf{q}} \left\langle \mathcal{D}_F^{(n-1)}(\mathbf{b}, \mathbf{q}) \mathcal{Q}(\mathbf{b}, \mathbf{K} - \mathbf{q}) \right\rangle_x. \quad (13)$$

*Numerical study.* We conclude this Letter with a numerical study of the sea quark TMDs at small  $x$ , with particular emphasis on  $xq^{(2)}$  and  $xq^{(3)}$  that have never been considered before. We rely on the mean field (or large- $N_c$ ) approximation, which allows us to factorise the CGC average in Eq. (13):  $\langle \mathcal{D}_F^{(n)} \mathcal{Q} \rangle \approx \langle \mathcal{D}_F^{(n)} \rangle \langle \mathcal{Q} \rangle$ . The basic building block is the dipole correlator, for which we use the McLerran-Venugopalan model [76, 77]. To study nuclear effects, we compare two types of targets: a dilute one (“proton”) with saturation momentum  $Q_{s0}^2 = 0.2 \text{ GeV}^2$  and a dense one (“nucleus”) with  $Q_s^2 = A^{1/3} Q_{s0}^2 = 1 \text{ GeV}^2$ , hence  $A^{1/3} = 5$ . Our results are presented in Fig. 6, with solid lines for a “nucleus” and dashed lines for a “proton”, and for  $n = 1, 2, 3$ . As visible in these plots, the TMDs have a perturbative power tail  $1/K_\perp^2$  at large  $K_\perp$  and saturate to  $N_c/(4\pi^4)$  at low momenta  $K_\perp \ll Q_s$  [16]. The saturation region extends with increasing the power  $n$ . This is best seen in the nucleus over proton ratio (normalised by  $A^{1/3}$ ) shown in the bottom plot: increasing  $n$  effectively yields a larger saturation scale and also a stronger deviation of the ratio from 1. This trend can be analytically understood from Eq. (13): for large  $q_\perp \gg Q_s$ , the dipole correlator is rapidly decaying,  $\langle \mathcal{D}_F^{(n)}(\mathbf{q}) \rangle \propto 1/q_\perp^4$ , while it is

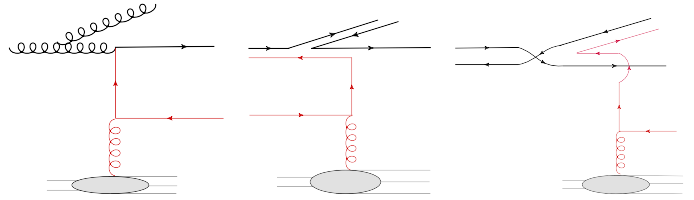


Figure 5. Target picture and large- $N_c$  colour flow for  $qg$  jets in gluon-initiated  $pA$  collisions: gluon emission by the gluon.

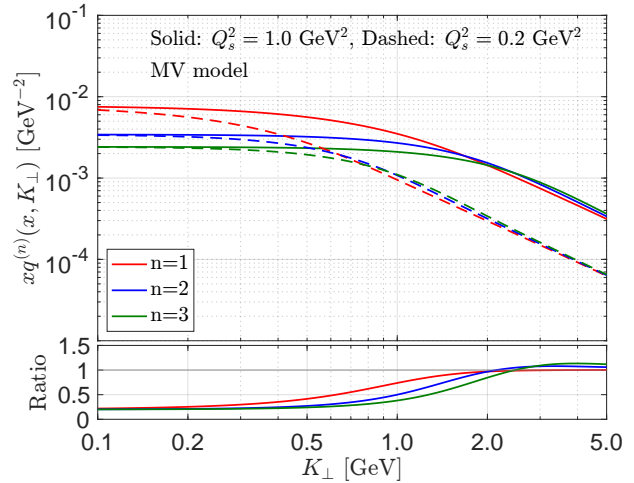


Figure 6. Small- $x$  quark TMD distributions for a proton and a nucleus with  $A^{1/3} = 5$ . Details in text.

roughly flat in the saturation region  $q_\perp^2 \lesssim nQ_s^2$ . Hence the integral in Eq. (13) is controlled by  $q_\perp^2 \lesssim nQ_s^2$  and this region extends when increasing  $n$ .

*Conclusion.* We have proven sea quark TMD factorisation for various back-to-back dijet processes at high energy from the CGC. The sea quark TMDs have a universal structure, which is built from the fundamental sea quark TMD involved in SIDIS/Drell-Yan at small  $x$  and the quark-antiquark dipole correlator. This structure agrees with the gauge link structure of the quark TMDs depending on the underlying hard partonic process, and in particular on the color flow of the external legs not attached to the TMD. These results pave the way towards the systematic incorporation of sea quark effects in the correlation limit of small  $x$  processes, a feature which has been largely overlooked in phenomenological works so far. For applications to the phenomenology, it is important to also take into account the additional, soft gluon radiation in the final state, which could strongly modify the back-to-back two-particle correlations. This can be done with the help of the Sudakov resummation method as developed in the CGC formalism [20, 21, 50, 71, 78–85] or, alternatively, by coupling to parton showers [86–88].

**Acknowledgements.** We are grateful to Xiaoxuan Chu, Larry McLerran, Yacine Mehtar-Tani, Al Mueller,

Björn Schenke and Raju Venugopalan for discussions. We thank the France-Berkeley-Fund from University of California at Berkeley for support. F.S. is supported by the Laboratory Directed Research and Development of Brookhaven National Laboratory and RIKEN- BNL Research Center. Part of this work was conducted while F.S. was supported by the Institute for Nuclear Theory's U.S. DOE under Grant No. DE-FG02-00ER41132. This work is supported in part by the U.S. Department of Energy, Office of Science, Office of Nuclear Physics, under contract number DE-AC02-05CH11231 (F.Y.), under the umbrella of the Quark-Gluon Tomography (QGT) Topical Collaboration with Award DE-SC0023646. P.C., E.I. and F.S. are grateful for the support of the Saturated Glue (SURGE) Topical Theory Collaboration, funded by the U.S. Department of Energy, Office of Science, Office of Nuclear Physics.

### Total amplitude for gluon-quark dijets in gluon-initiated pA collisions

The total amplitude receives contributions from 9 diagrams, which can be classified into three types according to the gluon emitter: quark ( $f = q$ ), antiquark ( $f = \bar{q}$ ), or gluon ( $f = g$ ) parent. At LP in  $K_{\perp}/P_{\perp}$  the total amplitude reads:

$$\mathcal{M}_{qg(\bar{q})}^{\lambda\bar{\lambda}\sigma\bar{\sigma}ab} = 8g^2q^+ \sqrt{z_q z} \frac{P^k}{P^2} \sum_{f=q,\bar{q},g} \Gamma_{f,jk}^{\lambda\bar{\lambda}\sigma\bar{\sigma}} \times \int \frac{d^2\ell}{(2\pi)^2} C_f^{ab}(\mathbf{K} - \ell, \mathbf{k} + \ell) \frac{\ell^j}{z M_{qg}^2 + \ell^2}, \quad (14)$$

where  $\sigma, \bar{\sigma}, \lambda, \bar{\lambda}$  respectively refer to the incoming and outgoing quark helicities and to the incoming and outgoing gluon polarisations, and  $a, b$  to the colours of incoming and outgoing gluons.  $j, k$  are transverse indices and  $M_{qg}$  is the invariant mass of the  $qg$ -dijet. The corresponding splitting functions are:

$$\begin{aligned} \Gamma_{q,jk}^{\lambda\bar{\lambda}\sigma\bar{\sigma}} &= -\delta^{\sigma,-\bar{\sigma}} \delta^{\sigma,-\lambda} (z_q \delta^{\sigma,\bar{\lambda}} + \delta^{\sigma,-\bar{\lambda}}) \epsilon_k^{\bar{\lambda}} \epsilon_j^{\lambda}, \\ \Gamma_{\bar{q},jk}^{\lambda\bar{\lambda}\sigma\bar{\sigma}} &= \delta^{\sigma,-\bar{\sigma}} \delta^{\bar{\sigma},-\bar{\lambda}} (z_q \delta^{\bar{\sigma},\lambda} - z_g \delta^{\bar{\sigma},-\lambda}) \epsilon_k^{\lambda} \epsilon_j^{\bar{\lambda}}, \\ \Gamma_{g,jk}^{\lambda\bar{\lambda}\sigma\bar{\sigma}} &= z_g \delta^{\sigma,-\bar{\sigma}} \left[ \frac{\delta^{\lambda,\bar{\lambda}} \epsilon_k^{\sigma}}{z_q} + \frac{\delta^{\lambda,-\sigma} \epsilon_k^{\bar{\lambda}*}}{z_g} - \delta^{\bar{\lambda},\sigma} \epsilon_k^{\lambda} \right] \epsilon_j^{\sigma*}, \end{aligned} \quad (15)$$

and the colour operators

$$\begin{aligned} C_q^{ab}(\mathbf{q}_1, \mathbf{q}_2) &= \int_{\mathbf{x}, \mathbf{y}} e^{-i\mathbf{q}_1 \cdot \mathbf{x}} e^{-i\mathbf{q}_2 \cdot \mathbf{y}} [t^b V_{\mathbf{x}} t^a V_{\mathbf{y}}^{\dagger} - U_{\mathbf{x}}^{ca} t^b t^c], \\ C_{\bar{q}}^{ab}(\mathbf{q}_1, \mathbf{q}_2) &= \int_{\mathbf{x}, \mathbf{y}} e^{-i\mathbf{q}_1 \cdot \mathbf{x}} e^{-i\mathbf{q}_2 \cdot \mathbf{y}} [U_{\mathbf{x}}^{bc} V_{\mathbf{x}} t^a t^c V_{\mathbf{y}}^{\dagger} - U_{\mathbf{x}}^{ca} t^c t^b], \\ C_g^{ab}(\mathbf{q}_1, \mathbf{q}_2) &= C_q^{ab}(\mathbf{q}_1, \mathbf{q}_2) - C_{\bar{q}}^{ab}(\mathbf{q}_1, \mathbf{q}_2). \end{aligned} \quad (16)$$

Note that the colour operator for the gluon emission from gluon can be written in terms of those for gluon

emission from quark and antiquark as anticipated from our heuristic discussion at large  $N_c$  (cf. Fig. 5).

\* caucal@subatech.in2p3.fr

† marcos.guerrero.morales@temple.edu

‡ edmond.iancu@ipht.fr

§ farid.salazar@temple.edu

¶ fyuan@lbl.gov

- [1] M. Derrick *et al.* (ZEUS), *Phys. Lett. B* **316**, 412 (1993).
- [2] E. Iancu, A. Leonidov, and L. McLerran, in *Cargese Summer School on QCD Perspectives on Hot and Dense Matter* (2002) pp. 73–145, [arXiv:hep-ph/0202270](#).
- [3] E. Iancu and R. Venugopalan, "The Color glass condensate and high-energy scattering in QCD," in *Quark-gluon plasma 4*, edited by R. C. Hwa and X.-N. Wang (2003) pp. 249–3363, [arXiv:hep-ph/0303204](#).
- [4] F. Gelis, E. Iancu, J. Jalilian-Marian, and R. Venugopalan, *Ann. Rev. Nucl. Part. Sci.* **60**, 463 (2010), [arXiv:1002.0333 \[hep-ph\]](#).
- [5] Y. V. Kovchegov and E. Levin, *Quantum Chromodynamics at High Energy*, Vol. 33 (Oxford University Press, 2013).
- [6] A. Morreale and F. Salazar, *Universe* **7**, 312 (2021), [arXiv:2108.08254 \[hep-ph\]](#).
- [7] A. Accardi *et al.*, *Eur. Phys. J. A* **52**, 268 (2016), [arXiv:1212.1701 \[nucl-ex\]](#).
- [8] R. Abdul Khalek *et al.*, *Nucl. Phys. A* **1026**, 122447 (2022), [arXiv:2103.05419 \[physics.ins-det\]](#).
- [9] P. Achenbach *et al.*, *Nucl. Phys. A* **1047**, 122874 (2024), [arXiv:2303.02579 \[hep-ph\]](#).
- [10] A. M. Stasto, K. J. Golec-Biernat, and J. Kwiecinski, *Phys. Rev. Lett.* **86**, 596 (2001), [arXiv:hep-ph/0007192](#).
- [11] C. Marquet and L. Schoeffel, *Phys. Lett. B* **639**, 471 (2006), [arXiv:hep-ph/0606079](#).
- [12] J. Breitweg *et al.* (ZEUS), *Eur. Phys. J. C* **7**, 609 (1999), [arXiv:hep-ex/9809005](#).
- [13] C. Adloff *et al.* (H1), *Nucl. Phys. B* **497**, 3 (1997), [arXiv:hep-ex/9703012](#).
- [14] L. D. McLerran and R. Venugopalan, *Phys. Rev. D* **59**, 094002 (1999), [arXiv:hep-ph/9809427](#).
- [15] R. Venugopalan, *Acta Phys. Polon. B* **30**, 3731 (1999), [arXiv:hep-ph/9911371](#).
- [16] A. H. Mueller, *Nucl. Phys. B* **558**, 285 (1999), [arXiv:hep-ph/9904404](#).
- [17] J. Collins, *Foundations of Perturbative QCD*, Cambridge Monographs on Particle Physics, Nuclear Physics and Cosmology, Vol. 32 (Cambridge University Press, 2023).
- [18] R. Boussarie *et al.*, (2023), [arXiv:2304.03302 \[hep-ph\]](#).
- [19] C. Marquet, B.-W. Xiao, and F. Yuan, *Phys. Lett. B* **682**, 207 (2009), [arXiv:0906.1454 \[hep-ph\]](#).
- [20] B.-W. Xiao, F. Yuan, and J. Zhou, *Nucl. Phys. B* **921**, 104 (2017), [arXiv:1703.06163 \[hep-ph\]](#).
- [21] P. Caucal, E. Iancu, A. H. Mueller, and F. Yuan, *Phys. Rev. Lett.* **134**, 061903 (2025), [arXiv:2408.03129 \[hep-ph\]](#).
- [22] X.-B. Tong, B.-W. Xiao, and Y.-Y. Zhang, *Phys. Rev. Lett.* **130**, 151902 (2023), [arXiv:2211.01647 \[hep-ph\]](#).
- [23] Y. Hatta, B.-W. Xiao, and F. Yuan, *Phys. Rev. D* **106**, 094015 (2022), [arXiv:2205.08060 \[hep-ph\]](#).
- [24] S. Hauksson, E. Iancu, A. H. Mueller, D. N. Triantafyllopoulos, and S. Y. Wei, *JHEP* **06**, 180 (2024), [arXiv:2402.14748 \[hep-ph\]](#).

- [25] F. Dominguez, B.-W. Xiao, and F. Yuan, *Phys. Rev. Lett.* **106**, 022301 (2011), [arXiv:1009.2141 \[hep-ph\]](#).
- [26] F. Dominguez, C. Marquet, B.-W. Xiao, and F. Yuan, *Phys. Rev.* **D83**, 105005 (2011), [arXiv:1101.0715 \[hep-ph\]](#).
- [27] A. Metz and J. Zhou, *Phys. Rev. D* **84**, 051503 (2011), [arXiv:1105.1991 \[hep-ph\]](#).
- [28] F. Dominguez, J.-W. Qiu, B.-W. Xiao, and F. Yuan, *Phys. Rev. D* **85**, 045003 (2012), [arXiv:1109.6293 \[hep-ph\]](#).
- [29] A. Dumitru, T. Lappi, and V. Skokov, *Phys. Rev. Lett.* **115**, 252301 (2015), [arXiv:1508.04438 \[hep-ph\]](#).
- [30] P. Kotko, K. Kutak, C. Marquet, E. Petreska, S. Sapeta, and A. van Hameren, *JHEP* **09**, 106 (2015), [arXiv:1503.03421 \[hep-ph\]](#).
- [31] C. Marquet, E. Petreska, and C. Roiesnel, *JHEP* **10**, 065 (2016), [arXiv:1608.02577 \[hep-ph\]](#).
- [32] C. Marquet, C. Roiesnel, and P. Taels, *Phys. Rev. D* **97**, 014004 (2018), [arXiv:1710.05698 \[hep-ph\]](#).
- [33] A. Stasto, S.-Y. Wei, B.-W. Xiao, and F. Yuan, *Phys. Lett. B* **784**, 301 (2018), [arXiv:1805.05712 \[hep-ph\]](#).
- [34] J. L. Albacete, G. Giacalone, C. Marquet, and M. Matas, *Phys. Rev. D* **99**, 014002 (2019), [arXiv:1805.05711 \[hep-ph\]](#).
- [35] A. Dumitru, V. Skokov, and T. Ullrich, *Phys. Rev. C* **99**, 015204 (2019), [arXiv:1809.02615 \[hep-ph\]](#).
- [36] T. Altinoluk, R. Boussarie, C. Marquet, and P. Taels, *JHEP* **07**, 079 (2019), [arXiv:1810.11273 \[hep-ph\]](#).
- [37] H. Mäntysaari, N. Mueller, F. Salazar, and B. Schenke, *Phys. Rev. Lett.* **124**, 112301 (2020), [arXiv:1912.05586 \[nucl-th\]](#).
- [38] T. Altinoluk and R. Boussarie, *JHEP* **10**, 208 (2019), [arXiv:1902.07930 \[hep-ph\]](#).
- [39] R. Boussarie and Y. Mehtar-Tani, *Phys. Lett. B* **831**, 137125 (2022), [arXiv:2006.14569 \[hep-ph\]](#).
- [40] T. Altinoluk, R. Boussarie, C. Marquet, and P. Taels, *JHEP* **07**, 143 (2020), [arXiv:2001.00765 \[hep-ph\]](#).
- [41] R. Boussarie, H. Mäntysaari, F. Salazar, and B. Schenke, *JHEP* **09**, 178 (2021), [arXiv:2106.11301 \[hep-ph\]](#).
- [42] E. Iancu, A. H. Mueller, D. N. Triantafyllopoulos, and S. Y. Wei, *JHEP* **10**, 103 (2022), [arXiv:2207.06268 \[hep-ph\]](#).
- [43] S. Benić, O. Garcia-Montero, and A. Perkov, *Phys. Rev. D* **105**, 114052 (2022), [arXiv:2203.01685 \[hep-ph\]](#).
- [44] F. Deganutti, C. Royon, and S. Schlichting, *JHEP* **01**, 159 (2024), [arXiv:2311.01965 \[hep-ph\]](#).
- [45] I. Ganguli, A. van Hameren, P. Kotko, and K. Kutak, *Eur. Phys. J. C* **83**, 868 (2023), [arXiv:2306.04706 \[hep-ph\]](#).
- [46] A. van Hameren, H. Kakkad, P. Kotko, K. Kutak, and S. Sapeta, *Eur. Phys. J. C* **83**, 947 (2023), [arXiv:2306.17513 \[hep-ph\]](#).
- [47] V. Cheung, Z.-B. Kang, F. Salazar, and R. Vogt, *Phys. Rev. D* **110**, 094039 (2024), [arXiv:2409.04080 \[hep-ph\]](#).
- [48] P. Kotko, K. Kutak, S. Sapeta, A. M. Stasto, and M. Strikman, *Eur. Phys. J. C* **77**, 353 (2017), [arXiv:1702.03063 \[hep-ph\]](#).
- [49] E. Iancu, A. H. Mueller, and D. N. Triantafyllopoulos, *Phys. Rev. Lett.* **128**, 202001 (2022), [arXiv:2112.06353 \[hep-ph\]](#).
- [50] P. Caucal and E. Iancu, (2024), [arXiv:2406.04238 \[hep-ph\]](#).
- [51] J.-W. Qiu, W. Vogelsang, and F. Yuan, *Phys. Rev. D* **76**, 074029 (2007), [arXiv:0706.1196 \[hep-ph\]](#).
- [52] C. J. Bomhof, P. J. Mulders, and F. Pijlman, *Eur. Phys. J. C* **47**, 147 (2006), [arXiv:hep-ph/0601171](#).
- [53] T. Altinoluk, N. Armesto, and G. Beuf, *Phys. Rev. D* **108**, 074023 (2023), [arXiv:2303.12691 \[hep-ph\]](#).
- [54] T. Altinoluk, G. Beuf, and S. Mulani, (2024), [arXiv:2411.15047 \[hep-ph\]](#).
- [55] T. Altinoluk, G. Beuf, E. Blanco, and S. Mulani, (2024), [arXiv:2412.08485 \[hep-ph\]](#).
- [56] B. Z. Kopeliovich, L. I. Lapidus, and A. B. Zamolodchikov, *JETP Lett.* **33**, 595 (1981).
- [57] G. Bertsch, S. J. Brodsky, A. S. Goldhaber, and J. F. Gunion, *Phys. Rev. Lett.* **47**, 297 (1981).
- [58] A. H. Mueller, *Nucl. Phys.* **B335**, 115 (1990).
- [59] N. N. Nikolaev and B. Zakharov, *Z. Phys.* **C49**, 607 (1991).
- [60] P. Caucal and F. Salazar, (2025), [arXiv:2502.02634 \[hep-ph\]](#).
- [61] I. Kolbé, K. Roy, F. Salazar, B. Schenke, and R. Venugopalan, *JHEP* **01**, 052 (2021), [arXiv:2008.04372 \[hep-ph\]](#).
- [62] I. Balitsky, *Nucl. Phys.* **B463**, 99 (1996), [arXiv:hep-ph/9509348](#).
- [63] Y. V. Kovchegov, *Phys. Rev.* **D60**, 034008 (1999), [arXiv:hep-ph/9901281](#).
- [64] J. Jalilian-Marian, A. Kovner, A. Leonidov, and H. Weigert, *Nucl. Phys.* **B504**, 415 (1997), [arXiv:hep-ph/9701284](#).
- [65] J. Jalilian-Marian, A. Kovner, A. Leonidov, and H. Weigert, *Phys. Rev.* **D59**, 014014 (1998), [arXiv:hep-ph/9706377 \[hep-ph\]](#).
- [66] A. Kovner, J. G. Milhano, and H. Weigert, *Phys. Rev.* **D62**, 114005 (2000), [arXiv:hep-ph/0004014](#).
- [67] H. Weigert, *Nucl. Phys.* **A703**, 823 (2002), [arXiv:hep-ph/0004044](#).
- [68] E. Iancu, A. Leonidov, and L. D. McLerran, *Nucl. Phys.* **A692**, 583 (2001), [arXiv:hep-ph/0011241](#).
- [69] E. Iancu, A. Leonidov, and L. D. McLerran, *Phys. Lett.* **B510**, 133 (2001), [arXiv:hep-ph/0102009](#).
- [70] E. Ferreira, E. Iancu, A. Leonidov, and L. McLerran, *Nucl. Phys.* **A703**, 489 (2002), [arXiv:hep-ph/0109115](#).
- [71] T. Altinoluk, J. Jalilian-Marian, and C. Marquet, *Phys. Rev. D* **110**, 094056 (2024), [arXiv:2406.08277 \[hep-ph\]](#).
- [72] S. Catani and F. Hautmann, *Nucl. Phys.* **B427**, 475 (1994), [arXiv:hep-ph/9405388 \[hep-ph\]](#).
- [73] M. Ciafaloni and D. Colferai, *JHEP* **09**, 069 (2005), [arXiv:hep-ph/0507106](#).
- [74] F. Hautmann, M. Hentschinski, and H. Jung, *Nucl. Phys. B* **865**, 54 (2012), [arXiv:1205.1759 \[hep-ph\]](#).
- [75] M. Hentschinski, A. Kusina, K. Kutak, and M. Serino, *Eur. Phys. J. C* **78**, 174 (2018), [arXiv:1711.04587 \[hep-ph\]](#).
- [76] L. D. McLerran and R. Venugopalan, *Phys. Rev.* **D49**, 3352 (1994), [arXiv:hep-ph/9311205](#).
- [77] L. D. McLerran and R. Venugopalan, *Phys. Rev.* **D49**, 2233 (1994), [arXiv:hep-ph/9309289](#).
- [78] A. H. Mueller, B.-W. Xiao, and F. Yuan, *Phys. Rev. Lett.* **110**, 082301 (2013), [arXiv:1210.5792 \[hep-ph\]](#).
- [79] A. Mueller, B.-W. Xiao, and F. Yuan, *Phys. Rev. D* **88**, 114010 (2013), [arXiv:1308.2993 \[hep-ph\]](#).
- [80] Y. Hatta, B.-W. Xiao, F. Yuan, and J. Zhou, *Phys. Rev. D* **104**, 054037 (2021), [arXiv:2106.05307 \[hep-ph\]](#).
- [81] P. Taels, T. Altinoluk, G. Beuf, and C. Marquet, *JHEP* **10**, 184 (2022), [arXiv:2204.11650 \[hep-ph\]](#).
- [82] S. Mukherjee, V. V. Skokov, A. Tarasov, and S. Tiwari, *Phys. Rev. D* **109**, 034035 (2024), [arXiv:2311.16402 \[hep-ph\]](#).
- [83] P. Caucal, F. Salazar, B. Schenke, T. Stebel, and R. Venugopalan, *Phys. Rev. Lett.* **132**, 081902 (2024), [arXiv:2308.00022 \[hep-ph\]](#).
- [84] P. Caucal and F. Salazar, *JHEP* **12**, 130 (2024), [arXiv:2405.19404 \[hep-ph\]](#).
- [85] H. Duan, A. Kovner, and M. Lublinsky, (2024), [arXiv:2407.15960 \[hep-ph\]](#).

- [86] L. Zheng, E. Aschenauer, J. Lee, and B.-W. Xiao, *Phys. Rev. D* **89**, 074037 (2014), [arXiv:1403.2413 \[hep-ph\]](#).
- [87] A. van Hameren, *Comput. Phys. Commun.* **224**, 371 (2018), [arXiv:1611.00680 \[hep-ph\]](#).
- [88] K. Cassar, Z. Wang, X. Chu, and E.-C. Aschenauer, (2025), [arXiv:2503.08447 \[hep-ph\]](#).